

# NEUTRON STARS IN RELATIVISTIC MEAN FIELD THEORY WITH ISOVECTOR SCALAR MESON

S. Kubis<sup>a</sup>, M. Kutschera<sup>a,b</sup> and S. Stachniewicz<sup>a</sup>

<sup>a</sup> H.Niewodniczański Institute of Nuclear Physics  
ul. Radzikowskiego 152, 31-342 Kraków, Poland

<sup>b</sup> Institute of Physics, Jagellonian University  
ul. Reymonta 4, 30-059 Kraków, Poland

Abstract:

We study the equation of state (EOS) of  $\beta$ -stable dense matter and models of neutron stars in the relativistic mean field (RMF) theory with the isovector scalar mean field corresponding to the  $\delta$ -meson [ $a_0(980)$ ]. A range of values of the  $\delta$ -meson coupling compatible with the Bonn potentials is explored. Parameters of the model in the isovector sector are constrained to fit the nuclear symmetry energy,  $E_s \approx 30 \text{ MeV}$ . We find that the quantity most sensitive to the  $\delta$ -meson coupling is the proton fraction of neutron star matter. It increases significantly in the presence of the  $\delta$ -field. The energy per baryon also increases but the effect is smaller. The EOS becomes slightly stiffer and the maximum neutron star mass increases for stronger  $\delta$ -meson coupling.

PACS: 21.65.+f, 97.60.Jd

## 1. Nucleon matter in the RMF model with the $\delta$ -meson

The standard RMF model [1] of nuclear matter, frequently used in astrophysical calculations, involves mean fields of  $\sigma$ ,  $\omega$  and  $\rho$  mesons. It does not include the contribution of the isovector scalar meson  $\delta$  [ $a_0(980)$ ] although generally the density to which this field can couple does not vanish,  $\langle \bar{\psi} \tau_3 \psi \rangle \neq 0$ . The contribution of the  $\delta$ -meson field is not expected to be important for finite nuclei of small isospin-asymmetry, as the  $\delta$ -meson mean field vanishes in symmetric nuclear matter. However, for strongly isospin-asymmetric matter in neutron stars presence of the  $\delta$ -field can influence the properties of dense matter. In Ref.[2] the RMF model was generalized to include the contribution of the  $\delta$ -meson. Here we investigate consequences of such a generalized RMF theory for neutron stars.

The dynamics of the RMF model is governed by the lagrangian

$$L = L_0 + L_{int}, \quad (1)$$

where  $L_0 = L_\psi + L_\sigma + L_\omega + L_\rho + L_\delta$  is the free-field lagrangian and  $L_{int}$  is the interaction term. The free-field lagrangians for nucleons and meson fields are:

$$L_\psi = \bar{\psi}(i\partial_\mu\gamma^\mu - m)\psi, \quad (2)$$

where  $m$  is the bare nucleon mass,

$$L_\sigma = \frac{1}{2}(\partial_\mu\sigma\partial^\mu\sigma - m_\sigma^2\sigma^2), \quad (3)$$

$$L_\omega = -\frac{1}{4}(\partial_\mu\omega_\nu - \partial_\nu\omega_\mu)(\partial^\mu\omega^\nu - \partial^\nu\omega^\mu) + \frac{1}{2}m_\omega^2\omega_\mu\omega^\mu, \quad (4)$$

$$L_\rho = -\frac{1}{4}(\partial_\mu\vec{\rho}_\nu - \partial_\nu\vec{\rho}_\mu)(\partial^\mu\vec{\rho}^\nu - \partial^\nu\vec{\rho}^\mu) + \frac{1}{2}m_\rho^2\vec{\rho}_\mu\vec{\rho}^\mu. \quad (5)$$

Here  $m_\sigma$ ,  $m_\omega$ , and  $m_\rho$  are masses of respective mesons. Lagrangians (2)-(5) are the same as used in the standard RMF theory [1].

For the  $\delta$ -field we use the simplest lagrangian of the massive isovector scalar field,

$$L_\delta = \frac{1}{2}\partial_\mu\vec{\delta}\partial^\mu\vec{\delta} - \frac{1}{2}m_\delta^2\vec{\delta}^2, \quad (6)$$

where  $m_\delta$  is the mass of the  $\delta$ -meson.

The coupling of the meson fields to nucleons is assumed to have the Yukawa form. For the  $\sigma$ -field we use the cubic and quartic selfinteraction terms. The interaction lagrangian reads

$$L_{int} = g_\sigma\sigma\bar{\psi}\psi - g_\omega\omega_\mu\bar{\psi}\gamma^\mu\psi - \frac{1}{2}g_\rho\vec{\rho}_\mu\bar{\psi}\gamma^\mu\vec{\tau}\psi + g_\delta\vec{\delta}\bar{\psi}\vec{\tau}\psi - U(\sigma), \quad (7)$$

where  $U(\sigma)$  is the potential energy term of the  $\sigma$ -field due to Boguta and Bodmer [3],

$$U(\sigma) = \frac{1}{3}bm\sigma^3 + \frac{1}{4}c\sigma^4. \quad (8)$$

In the RMF approximation, for a uniform nucleon matter only a few fermion densities are relevant. These include the baryon density,  $\langle \bar{\psi}\gamma_0\psi \rangle = n_B$ , the scalar density,  $\langle \bar{\psi}\psi \rangle$ , the isospin density,  $\langle \bar{\psi}\gamma_0\tau_3\psi \rangle$ , and the scalar isospin density,  $\langle \bar{\psi}\tau_3\psi \rangle$ . A selfconsistent description of the system is achieved by taking into account only those components of the meson fields which couple to the above densities with all remaining components vanishing. For normal nucleon matter the relevant components of mean meson fields are  $\bar{\sigma}$ ,  $\bar{\omega}_0$ ,  $\bar{\rho}_0^{(3)}$ , and, for the  $\delta$ -field, the isospin component  $\bar{\delta}^{(3)}$ .

It is a simple algebraic exercise to obtain the spectrum of nucleon energies in terms of the above components of meson fields and to construct all relevant nucleon densities. The single particle energies of protons and neutrons are

$$E_{P(N)}(\mathbf{p}) = g_\omega\bar{\omega}_0 \pm \frac{1}{2}g_\rho\bar{\rho}_0^{(3)} + \sqrt{\mathbf{p}^2 + m_{P(N)}^2}, \quad (9)$$

where the proton and neutron effective mass is, respectively,

$$m_P = m - g_\sigma\bar{\sigma} - g_\delta\bar{\delta}^{(3)}, \quad (10)$$

and

$$m_N = m - g_\sigma \bar{\sigma} + g_\delta \bar{\delta}^{(3)}. \quad (11)$$

The plus (minus) sign in the formula (9) refers to protons (neutrons).

We obtain the field equations for mean meson fields in the form:

$$m_\omega^2 \bar{\omega}_0 = g_\omega n_B, \quad (12)$$

$$m_\rho^2 \bar{\rho}_0^{(3)} = \frac{1}{2} g_\rho (2x - 1) n_B, \quad (13)$$

where  $x = n_P/n_B$  is the proton fraction,

$$m_\sigma^2 \bar{\sigma} + \frac{\partial U}{\partial \sigma} = g_\sigma (n_P^s + n_N^s), \quad (14)$$

and

$$m_\delta^2 \bar{\delta}^{(3)} = g_\delta (n_P^s - n_N^s). \quad (15)$$

In Eqs.(14) and (15)  $n_P^s$  and  $n_N^s$  is, respectively, proton and neutron scalar density,

$$n_i^s = \frac{2}{(2\pi)^3} \int_0^{k_i} d^3 k \frac{m_i}{\sqrt{k^2 + m_i^2}}, \quad i = P, N, \quad (16)$$

with proton and neutron effective mass,  $m_P$  and  $m_N$ , given in Eqs.(10) and (11). Mean meson fields as determined through Eqs.(12)-(15) depend on the baryon density  $n_B$  and the proton fraction  $x$ .

The energy of the uniform matter consists of nucleon and meson contributions. The nucleon contribution is a sum of proton and neutron energies (9) up to their respective Fermi momenta. Mean meson field contributions are easily obtained from the lagrangians (4)-(6). With the mean meson fields given by Eqs.(12)-(15) the energy density of a uniform nucleon matter becomes

$$\begin{aligned} \epsilon_{nuc} = & \frac{2}{(2\pi)^3} \left( \int^{k_P} d^3 k \sqrt{k^2 + m_P^2} + \int^{k_N} d^3 k \sqrt{k^2 + m_N^2} \right) + \frac{1}{2} C_\omega^2 n_B^2 + \\ & + \frac{1}{2} \frac{1}{C_\sigma^2} \left[ m - \frac{m_P + m_N}{2} \right]^2 + U(\bar{\sigma}) + \frac{1}{8} C_\rho^2 (2x - 1)^2 n_B^2 + \frac{1}{8} \frac{1}{C_\delta^2} (m_N - m_P)^2. \end{aligned} \quad (17)$$

In the spirit of the RMF theory [1] the parameters of the model are fit to reproduce the empirical parameters of nuclear matter. In the isoscalar sector, the coupling parameters,  $C_\sigma^2 \equiv g_\sigma^2/m_\sigma^2$ ,  $C_\omega^2 \equiv g_\omega^2/m_\omega^2$ ,  $\bar{b} \equiv b/g_\sigma^3$ , and  $\bar{c} \equiv c/g_\sigma^4$ , are adjusted to fit the saturation properties of symmetric nuclear matter ( $x = 1/2$ ), i.e. the saturation density  $n_0 = 0.145 fm^{-3}$ , the binding energy  $B = -16 MeV$  per nucleon, and the compressibility

modulus  $K_V \approx 280 \text{ MeV}$ . The fourth parameter, e.g.  $\bar{c}$ , can be used to control the stiffness of the equation of state of symmetric nuclear matter. Our choice of these coupling parameters is discussed below.

The coupling parameters,  $C_\rho^2 \equiv g_\rho^2/m_\rho^2$ , and  $C_\delta^2 \equiv g_\delta^2/m_\delta^2$ , in the isovector sector are constrained to fit the nuclear symmetry energy,  $E_s = 31 \pm 4 \text{ MeV}$  [4]. This constraint gives  $C_\rho^2$  as a function of  $C_\delta^2$  [2]. In the range of values of  $C_\delta^2$  considered below, which is compatible with the Bonn potentials [5], this function is well approximated by a linear relation [2]

$$C_\rho^2 = AC_\delta^2 + B, \quad (18)$$

with positive coefficients,  $A > 0$ , and  $B > 0$ , depending weakly on the coupling parameters in the isoscalar sector.

The requirement that the nuclear symmetry energy is reproduced in the presence of the  $\delta$ -field is very important as the  $\delta$ -field contribution is strongly attractive. As shown in Ref.[2] the  $\delta$ -meson coupling provides a negative contribution to the symmetry energy that tends to cancel partially the  $\rho$ -meson contribution. Thus to preserve the nuclear symmetry energy a stronger  $\rho$ -meson coupling is needed. The formula (18) shows that the parameter  $C_\rho^2$  has the lowest value  $C_\rho^2 = B$  for  $C_\delta^2 = 0$ . For any coupling constant  $C_\delta^2 > 0$ , the value of the  $\rho$ -coupling constant,  $C_\rho^2$ , increases. Hence for pure neutron matter inclusion of the  $\delta$ -meson results unavoidably in higher energy per particle at high densities, where contributions of vector mesons dominate.

## 2. Equation of state and neutron stars

As we mentioned above, there is one parameter, e.g.  $\bar{c}$ , which can be used to label a family of EOS's in the RMF model. We wish to retain this freedom, as the true high density behaviour of the neutron star EOS is only weakly constrained at present [6]. In the following we shall mainly use two sets of coupling parameters which reproduce the saturation properties of nuclear matter but predict different stiffness of the EOS at higher densities. The EOS's corresponding to these two sets of parameters are referred to as soft and stiff. The soft EOS is specified by the parameters  $C_\sigma^2 = 1.582 \text{ fm}^2$ ,  $C_\omega^2 = 1.019 \text{ fm}^2$ ,  $\bar{b} = -0.7188$ , and  $\bar{c} = 6.563$ . For the stiff EOS the parameters are  $C_\sigma^2 = 11.25 \text{ fm}^2$ ,  $C_\omega^2 = 6.483 \text{ fm}^2$ ,  $\bar{b} = 0.003825$ , and  $\bar{c} = 3.5 \times 10^{-6}$ .

The above EOS's limit in a sense the family of EOS's in the RMF model. They are close to the softest and to the stiffest EOS in the RMF theory that are physically allowed. The stiff EOS corresponds to a very small value of the parameter  $\bar{c}$ . Physical consistency of the RMF theory requires that  $\bar{c} > 0$ . In Fig.1 we show a plot of the parameter  $\bar{c}$  as a function of  $C_\sigma^2$ . As one can see,  $\bar{c} = 0$  for  $C_\sigma^2 \approx 11.5 \text{ fm}^2$  and thus any acceptable value of  $C_\sigma^2$  must be lower (Fig.1). In terms of the maximum neutron star mass, the EOS with  $\bar{c} \rightarrow 0$  is the stiffest acceptable EOS in the RMF model. We choose small but finite value  $\bar{c} = 3.5 \times 10^{-6}$  with corresponding  $C_\sigma^2 = 11.25 \text{ fm}^2$ .

The parameter  $\bar{c}$  for the soft EOS has the highest allowed value,  $\bar{c} = 6.563$ . The maximum neutron star mass corresponding to this EOS is about  $1.44 M_\odot$ . This is the mass of the heavier neutron star in the binary pulsar PSR B1913+16 [7], which has the

largest precisely measured value of a neutron star mass. Hence this EOS is the softest one still compatible with measured neutron star masses.

We also show below some results for an intermediate EOS with the parameters  $C_\sigma^2 = 5.318fm^2$ ,  $C_\omega^2 = 2.31fm^2$ ,  $\bar{b} = -0.03952$ , and  $\bar{c} = 0.4229$ .

The coupling constant  $g_\delta$  of the  $\delta$ -nucleon interaction is a parameter in the one-boson-exchange fits of nucleon-nucleon scattering data. Its value is not, however, strongly constrained at present [5]. Our aim in this paper is to investigate the influence of this coupling parameter on the EOS of dense matter and on properties of neutron stars. To do so we adopt here a range of the  $\delta$ -meson coupling compatible with the Bonn potentials [5],  $C_\delta^2 \leq 4.4fm^2$ . The maximum value of  $C_\delta^2$  we use exceeds the value corresponding to the Bonn potential C [5] which is  $C_\delta^2 \approx 2.5fm^2$ .

For a given  $\delta$ -coupling,  $C_\delta^2$ , we obtain the  $\rho$ -meson coupling,  $C_\rho^2$ , from Eq.(18) applying for the soft EOS the coefficients  $A = 0.63$  and  $B = 5.0fm^2$ . For the stiff EOS, the coefficients in Eq.(18) are  $A = 0.60$  and  $B = 4.31fm^2$ .

To obtain the EOS of the neutron star matter we first calculate the proton fraction  $x$  of the charge-neutral  $\beta$ -stable neutron star matter, which satisfies the condition

$$\mu_N - \mu_P = \sqrt{k_N^2 + m_N^2} - \sqrt{k_P^2 + m_P^2} + \frac{1}{2}C_\rho^2(1 - 2x)n_B = \mu_e = \mu_\mu, \quad (19)$$

where  $\mu_e = k_e = (3\pi^2n_e)^{1/3}$  is the electron chemical potential and  $\mu_\mu = \sqrt{k_\mu^2 + m_\mu^2}$  is the muon chemical potential. Charge neutrality requires that  $n_e + n_\mu = n_P = xn_B$ .

In Fig.2 we show the proton fraction  $x$  as a function of density for a few values of  $C_\delta^2$ . One can notice that for both EOS's the proton fraction is substantially larger for indicated values of the  $\delta$ -meson coupling,  $C_\delta^2$ , than for vanishing coupling,  $C_\delta^2 = 0$ . It exceeds the critical value for the direct URCA process to dominate the cooling rate of neutron stars, which is  $x_{URCA} \approx 0.11$ , already at densities less than twice the nuclear saturation density. For the stiff EOS and for the  $\delta$ -coupling corresponding to the Bonn potential C,  $C_\delta^2 = 2.5fm^2$ , the proton fraction is about 40% higher than for vanishing  $\delta$ -meson coupling. For the soft EOS the proton fraction increases by about 20%, a somewhat weaker effect.

The energy density of the  $\beta$ -stable neutron star matter,  $\epsilon_{ns}$ , is obtained as a sum of nucleon and lepton contributions,

$$\epsilon_{ns} = \epsilon_{nuc} + \frac{1}{4\pi^2}k_e^4 + \frac{2}{(2\pi)^3} \int_0^{k_\mu} d^3k \sqrt{k^2 + m_\mu^2}, \quad (20)$$

where nucleon contribution,  $\epsilon_{nuc}$ , is given in Eq.(17). Next terms represent the energy density of the electron Fermi sea and the muon Fermi sea. The energy per baryon with the contribution of the  $\delta$ -field for both soft and stiff EOS is shown in Fig.3. For comparison, curves with no  $\delta$ -field included are also shown. As one can see in Fig.3 the energy per particle increases with  $\delta$ -coupling  $C_\delta^2$ . The effect is stronger for the stiff EOS. For  $C_\delta^2 = 2.5fm^2$  the energy per baryon is about 10% higher than for  $C_\delta^2 = 0$ . For the soft EOS the energy per baryon increases by  $\sim 5\%$ .

It is interesting to note that actually the nucleon contribution to the energy per baryon at a given  $n_B$  decreases with increasing  $C_\delta^2$  for both EOS's. It is the lepton contribution which makes the total energy per particle higher.

This behaviour can be easily understood. With increasing  $C_\delta^2$  the proton fraction of the neutron star matter in  $\beta$ -equilibrium increases making the system less isospin-asymmetric. This in turn reduces the amplitude of the  $\rho$ -meson mean field,  $\bar{\rho}_0^{(3)}$ , which provides a repulsive contribution. As a result, the nucleon energy per baryon is lowered in spite of the fact that the  $\rho$ -meson coupling parameter,  $C_\rho^2$ , is higher. However, increase of the proton fraction results in higher density of electrons and muons which thus contribute more to the total energy per particle. The energy per baryon of the  $\beta$ -stable neutron star matter displays a similar behaviour as the one of pure neutron matter which becomes higher with increasing  $\delta$ -meson coupling [2].

In Fig.4 pressure as a function of mass density,  $P = P(\epsilon/c^2)$ , a relation referred to as the EOS of neutron star matter, is shown. In this plot curves corresponding to  $C_\delta^2 = 4.4fm^2$  and to  $C_\delta = 0$  differ significantly for both soft and stiff EOS. Pressure at a given mass density is higher for  $C_\delta^2 = 4.4fm^2$  than for  $C_\delta^2 = 0$  which indicates that the EOS becomes somewhat stiffer when the  $\delta$ -meson contribution is present.

The soft EOS and the stiff EOS calculated for  $C_\delta^2 = 2.5fm^2$ , a value corresponding to the Bonn potential C, are given in Table Ia and Table Ib, respectively. As the proton fraction at high densities is rather high, especially for the stiff EOS, leptons (electrons and muons) make a sizable contribution to the total mass density.

To gauge the influence of the  $\delta$ -meson coupling on the EOS we have calculated models of neutron stars. The high density EOS calculated in the previous section was matched with the low density EOS due to Baym, Bethe, and Pethick [8] by constructing a proper phase transition. By making this construction we have found interface between crust matter, described by the EOS of Ref.[8], and liquid core matter, described by our RMF theory. Both EOS's in Table Ia and Ib are given for liquid core matter starting from the core interface density.

In Fig.5 density profiles are shown for the canonical neutron star mass  $1.4M_\odot$ . For the soft EOS generally the radii are smaller than for the stiff EOS. The effect of the  $\delta$ -meson contribution is more profound in case of the soft EOS. The radius increases from  $R \approx 10.6km$ , for  $C_\delta^2 = 0$ , to  $R \approx 11.9km$ , for  $C_\delta^2 = 2.5fm^2$ , and to  $R \approx 12.5km$ , for  $C_\delta^2 = 4.4fm^2$ . For the stiff EOS the radius is  $R \approx 13.8km$  for  $C_\delta^2 = 0$ ,  $R \approx 14.2km$  for  $C_\delta^2 = 2.5fm^2$ , and  $R \approx 14.6km$ , for  $C_\delta^2 = 4.4fm^2$ . The central density decreases with increasing  $\delta$ -coupling. In case of the soft EOS, the central density is  $n_c \approx 8.5n_0$ ,  $n_c \approx 5.4n_0$  and  $n_c \approx 4.4n_0$  for, respectively,  $C_\delta^2 = 0$ ,  $C_\delta^2 = 2.5fm^2$  and  $C_\delta^2 = 4.4fm^2$ . For the stiff EOS corresponding central densities are  $n_c \approx 2.3n_0$ ,  $n_c \approx 2.1n_0$  and  $n_c \approx 1.9n_0$ , respectively.

It is interesting to study the core of  $1.4M_\odot$  neutron star models with the proton fraction exceeding the critical URCA value,  $x_{URCA}$ , where the direct URCA process dominates the cooling rate. With increasing  $C_\delta^2$  there are two effects influencing its size which tend to cancel one another: increase of the proton fraction at a given baryon density (Fig.2) and decrease of the central density  $n_c$  due to stiffening of the EOS. The former one tends to extend the core while the latter one tends to shrink it. As a result, the core size is rather

insensitive to changes of the  $\delta$ -coupling  $C_\delta^2$ . It is determined primarily by the stiffness of the EOS for  $C_\delta^2 = 0$ . Generally, the mass of the core where direct URCA process dominates is higher for the soft EOS than for the stiff EOS.

The neutron star mass as a function of central density is displayed in Fig.6 for the soft and the stiff EOS. We also show results for the intermediate EOS, with parameters given in Sect.2. Maximum mass increases slightly with  $C_\delta^2$ . The  $\delta$ -field plays a more important role for the soft EOS. The maximum neutron star mass is  $M_{max} = 1.403M_\odot$  for  $C_\delta^2 = 0$ . Since this value is less than the mass of the neutron star in the binary pulsar PSR B1913+16, which is  $1.44M_\odot$ , this EOS is too soft to be realistic. However, with inclusion of the  $\delta$ -field contribution the maximum neutron star mass increases to  $M_{max} = 1.452M_\odot$ , for  $C_\delta^2 = 2.5fm^2$ , and to  $M_{max} = 1.48M_\odot$ , for  $C_\delta^2 = 4.4fm^2$ . Inclusion of the  $\delta$ -meson with  $C_\delta^2 = 2.5fm^2$  results in about 4% increase of  $M_{max}$  that makes the soft EOS astrophysically acceptable.

For the stiff EOS the maximum neutron star mass is  $M_{max} = 2.275M_\odot$ ,  $M_{max} = 2.309M_\odot$  and  $M_{max} = 2.313M_\odot$  for, respectively,  $C_\delta^2 = 0$ ,  $C_\delta^2 = 2.5fm^2$  and  $C_\delta^2 = 4.4fm^2$ . In this case  $M_{max}$  increases by  $\sim 1.5\%$  for  $C_\delta^2 = 2.5fm^2$ . Central densities of the above maximum mass neutron stars are, respectively,  $n_c \approx 6.2n_0$ ,  $n_c \approx 5.9n_0$  and  $n_c \approx 5.7n_0$

### 3. Conclusions and discussion

We have studied the influence of the  $\delta$ -meson coupling on the EOS of neutron star matter in the RMF theory. When the isovector scalar field of the  $\delta$ -meson is added to the standard RMF model, the nuclear symmetry energy has two contributions of opposite sign. The conventional  $\rho$ -meson contribution is positive, whereas the  $\delta$ -meson contribution is negative [2]. This reflects the fact that in pure neutron matter the  $\rho$ -meson provides repulsion whereas the  $\delta$ -meson produces additional attraction. It is thus obvious that in order to make physically relevant predictions of the EOS of neutron star matter the coupling parameters of the  $\delta$  and  $\rho$  mesons to nucleons should be constrained in such a way that the empirical value of the nuclear symmetry is preserved.

We have found that the quantity most strongly affected by the presence of the  $\delta$ -field is the proton fraction of the neutron star matter in  $\beta$ -equilibrium. It increases rapidly with  $C_\delta^2$ . The effect is more profound for the stiff EOS, for which the proton fraction increases by  $\sim 40\%$  for the value of  $C_\delta^2 = 2.5fm^2$  corresponding to the Bonn potential C. For the soft EOS the proton fraction increases in this case by  $\sim 20\%$ . For higher values of the  $\delta$ -coupling parameter this increase is larger (Fig.2). The URCA threshold concentration of protons,  $x_{URCA} \approx 0.11$ , occurs at lower densities.

The  $\delta$ -field contribution makes the energy per baryon of  $\beta$ -stable neutron star matter higher by  $\sim 10\%$  and  $\sim 5\%$  for the stiff and soft EOS, respectively, and for the Bonn potential C value of  $C_\delta^2$ . Here the increase is due to larger leptonic contribution since the nucleon contribution actually decreases with  $C_\delta^2$ . The EOS with  $C_\delta^2 \neq 0$  is slightly stiffer than for  $C_\delta^2 = 0$ . Maximum mass of the neutron star also increases by a few percent.

One should stress that the extension of the RMF model to include the isovector scalar meson  $\delta$  is the most natural one. In fact, the standard RMF model with no  $\delta$ -field is not fully selfconsistent, as for isospin-asymmetric matter the density  $\langle \bar{\psi}\tau_3\psi \rangle \neq 0$  whereas the mean field with the same quantum numbers vanishes. The coupling constant  $g_\delta$  is not well determined at present [5]. However for values in the range compatible with the Bonn

potentials [5] the contribution of the  $\delta$ -field in pure neutron matter at saturation density is quite strong [2]. If the  $\rho$ -coupling is unchanged, the neutron matter becomes selfbound for  $C_\delta^2 \approx 1.0 fm^2$ . To avoid such an unphysical behaviour the  $\rho$ -coupling  $C_\rho^2$  should be readjusted to meet the requirement that the empirical value of the nuclear symmetry energy is reproduced.

## Acknowledgements

This research is partially supported by the Polish State Committee for Scientific Research (KBN), grants 2 P03D 001 09 and 2 P03B 083 08.

## References

- [1] B. D. Serot and J. D. Walecka, *Adv. Nucl. Phys.* **16** (1986) 1.
- [2] S. Kubis and M. Kutschera, *Phys.Lett.B* **399** (1997) 191.
- [3] J. Boguta and A. Bodmer, *Nucl. Phys.* **A292** (1977) 413.
- [4] W. D. Myers and W. D. Swiatecki, *Ann. Phys.* **84** (1973) 186;  
J. M. Pearson, Y. Aboussir, A. K. Dutta, R. C. Nayak, M. Farine, and F. Tondeur, *Nucl. Phys.* **A528** (1991) 1;  
P. Möller and J. R. Nix, *At. Data and Nucl. Data Tables* **39** (1988) 219;  
P. Möller, W. D. Myers, W. J. Swiatecki, and J. Treiner, *At. Data and Nucl. Data Tables* **39** (1988) 225;  
W. D. Myers, W. J. Swiatecki, T. Kodama, L. J. El-Jaick, and E. R. Hilf, *Phys. Rev.* **C15** (1977) 2032.
- [5] R. Machleidt, *Adv. Nucl. Phys.* **19** (1989) 189.
- [6] M. Kutschera, astro-ph/9612143, in "Solar Astrophysics, Structure of Neutron Stars, Gamma Flashes. Meeting of the Commission for Astrophysics of the Polish Academy of Arts and Sciences", ed. K. Grotowski, Cracow, 1997.
- [7] J. H. Taylor and J. M. Weisberg, *Astrophys. J.* **345** (1989) 434.
- [8] G. Baym, H. A. Bethe and C. J. Pethick, *Nucl. Phys.* **A175** (1971) 225.



Table Ia  
Soft equation of state,  $C_\delta^2 = 2.5 fm^2$

$n_B(cm^{-3})$	$\rho(g/cm^3)$	$P(dynes/cm^2)$
$8.320 \times 10^{37}$	$1.404 \times 10^{14}$	$1.612 \times 10^{31}$
$8.360 \times 10^{37}$	$1.411 \times 10^{14}$	$4.034 \times 10^{31}$
$8.400 \times 10^{37}$	$1.418 \times 10^{14}$	$6.487 \times 10^{31}$
$8.440 \times 10^{37}$	$1.425 \times 10^{14}$	$8.971 \times 10^{31}$
$8.481 \times 10^{37}$	$1.431 \times 10^{14}$	$1.148 \times 10^{32}$
$8.562 \times 10^{37}$	$1.445 \times 10^{14}$	$1.661 \times 10^{32}$
$8.603 \times 10^{37}$	$1.452 \times 10^{14}$	$1.922 \times 10^{32}$
$8.644 \times 10^{37}$	$1.459 \times 10^{14}$	$2.186 \times 10^{32}$
$8.686 \times 10^{37}$	$1.466 \times 10^{14}$	$2.454 \times 10^{32}$
$9.248 \times 10^{37}$	$1.561 \times 10^{14}$	$6.288 \times 10^{32}$
$1.013 \times 10^{38}$	$1.712 \times 10^{14}$	$1.303 \times 10^{33}$
$1.077 \times 10^{38}$	$1.821 \times 10^{14}$	$1.840 \times 10^{33}$
$1.217 \times 10^{38}$	$2.061 \times 10^{14}$	$3.161 \times 10^{33}$
$1.334 \times 10^{38}$	$2.263 \times 10^{14}$	$4.407 \times 10^{33}$
$1.462 \times 10^{38}$	$2.486 \times 10^{14}$	$5.877 \times 10^{33}$
$1.756 \times 10^{38}$	$3.003 \times 10^{14}$	$9.672 \times 10^{33}$
$1.924 \times 10^{38}$	$3.303 \times 10^{14}$	$1.211 \times 10^{34}$
$2.109 \times 10^{38}$	$3.634 \times 10^{14}$	$1.499 \times 10^{34}$
$2.321 \times 10^{38}$	$4.019 \times 10^{14}$	$1.858 \times 10^{34}$
$2.561 \times 10^{38}$	$4.457 \times 10^{14}$	$2.295 \times 10^{34}$
$2.825 \times 10^{38}$	$4.945 \times 10^{14}$	$2.816 \times 10^{34}$
$3.116 \times 10^{38}$	$5.491 \times 10^{14}$	$3.436 \times 10^{34}$
$3.437 \times 10^{38}$	$6.100 \times 10^{14}$	$4.175 \times 10^{34}$
$3.917 \times 10^{38}$	$7.026 \times 10^{14}$	$5.380 \times 10^{34}$
$4.321 \times 10^{38}$	$7.818 \times 10^{14}$	$6.485 \times 10^{34}$
$4.766 \times 10^{38}$	$8.705 \times 10^{14}$	$7.797 \times 10^{34}$
$5.258 \times 10^{38}$	$9.700 \times 10^{14}$	$9.355 \times 10^{34}$
$5.800 \times 10^{38}$	$1.081 \times 10^{15}$	$1.120 \times 10^{35}$
$6.619 \times 10^{38}$	$1.254 \times 10^{15}$	$1.426 \times 10^{35}$
$7.555 \times 10^{38}$	$1.456 \times 10^{15}$	$1.810 \times 10^{35}$
$8.250 \times 10^{38}$	$1.611 \times 10^{15}$	$2.121 \times 10^{35}$
$9.841 \times 10^{38}$	$1.974 \times 10^{15}$	$2.910 \times 10^{35}$
$1.123 \times 10^{39}$	$2.305 \times 10^{15}$	$3.686 \times 10^{35}$
$1.281 \times 10^{39}$	$2.696 \times 10^{15}$	$4.670 \times 10^{35}$
$1.463 \times 10^{39}$	$3.160 \times 10^{15}$	$5.917 \times 10^{35}$
$1.669 \times 10^{39}$	$3.711 \times 10^{15}$	$7.501 \times 10^{35}$
$1.905 \times 10^{39}$	$4.368 \times 10^{15}$	$9.515 \times 10^{35}$
$2.175 \times 10^{39}$	$5.154 \times 10^{15}$	$1.208 \times 10^{36}$

Table Ib  
Stiff equation of state,  $C_\delta^2 = 2.5 fm^2$

$n_B(cm^{-3})$	$\rho(g/cm^3)$	$P(dynes/cm^2)$
$3.190 \times 10^{37}$	$5.359 \times 10^{13}$	$8.324 \times 10^{29}$
$3.526 \times 10^{37}$	$5.924 \times 10^{13}$	$9.026 \times 10^{30}$
$3.898 \times 10^{37}$	$6.550 \times 10^{13}$	$2.364 \times 10^{31}$
$4.310 \times 10^{37}$	$7.242 \times 10^{13}$	$4.792 \times 10^{31}$
$4.765 \times 10^{37}$	$8.007 \times 10^{13}$	$8.641 \times 10^{31}$
$5.268 \times 10^{37}$	$8.853 \times 10^{13}$	$1.453 \times 10^{32}$
$6.438 \times 10^{37}$	$1.082 \times 10^{14}$	$3.625 \times 10^{32}$
$7.118 \times 10^{37}$	$1.197 \times 10^{14}$	$5.486 \times 10^{32}$
$7.869 \times 10^{37}$	$1.324 \times 10^{14}$	$8.135 \times 10^{32}$
$8.700 \times 10^{37}$	$1.465 \times 10^{14}$	$1.186 \times 10^{33}$
$1.044 \times 10^{38}$	$1.764 \times 10^{14}$	$2.282 \times 10^{33}$
$1.255 \times 10^{38}$	$2.125 \times 10^{14}$	$4.237 \times 10^{33}$
$1.375 \times 10^{38}$	$2.335 \times 10^{14}$	$5.702 \times 10^{33}$
$1.507 \times 10^{38}$	$2.566 \times 10^{14}$	$7.555 \times 10^{33}$
$1.652 \times 10^{38}$	$2.821 \times 10^{14}$	$9.925 \times 10^{33}$
$1.810 \times 10^{38}$	$3.104 \times 10^{14}$	$1.296 \times 10^{34}$
$1.984 \times 10^{38}$	$3.418 \times 10^{14}$	$1.683 \times 10^{34}$
$2.175 \times 10^{38}$	$3.766 \times 10^{14}$	$2.178 \times 10^{34}$
$2.399 \times 10^{38}$	$4.183 \times 10^{14}$	$2.855 \times 10^{34}$
$2.646 \times 10^{38}$	$4.652 \times 10^{14}$	$3.727 \times 10^{34}$
$2.919 \times 10^{38}$	$5.180 \times 10^{14}$	$4.846 \times 10^{34}$
$3.219 \times 10^{38}$	$5.777 \times 10^{14}$	$6.277 \times 10^{34}$
$3.551 \times 10^{38}$	$6.454 \times 10^{14}$	$8.102 \times 10^{34}$
$3.917 \times 10^{38}$	$7.225 \times 10^{14}$	$1.042 \times 10^{35}$
$4.321 \times 10^{38}$	$8.105 \times 10^{14}$	$1.338 \times 10^{35}$
$4.766 \times 10^{38}$	$9.114 \times 10^{14}$	$1.713 \times 10^{35}$
$5.258 \times 10^{38}$	$1.027 \times 10^{15}$	$2.188 \times 10^{35}$
$5.800 \times 10^{38}$	$1.161 \times 10^{15}$	$2.788 \times 10^{35}$
$6.619 \times 10^{38}$	$1.378 \times 10^{15}$	$3.852 \times 10^{35}$
$7.555 \times 10^{38}$	$1.643 \times 10^{15}$	$5.276 \times 10^{35}$
$8.622 \times 10^{38}$	$1.971 \times 10^{15}$	$7.183 \times 10^{35}$
$9.841 \times 10^{38}$	$2.381 \times 10^{15}$	$9.716 \times 10^{35}$
$1.123 \times 10^{39}$	$2.895 \times 10^{15}$	$1.304 \times 10^{36}$
$1.281 \times 10^{39}$	$3.542 \times 10^{15}$	$1.740 \times 10^{36}$
$1.463 \times 10^{39}$	$4.357 \times 10^{15}$	$2.307 \times 10^{36}$
$1.669 \times 10^{39}$	$5.390 \times 10^{15}$	$3.044 \times 10^{36}$
$1.905 \times 10^{39}$	$6.700 \times 10^{15}$	$4.000 \times 10^{36}$
$2.175 \times 10^{39}$	$8.366 \times 10^{15}$	$5.239 \times 10^{36}$

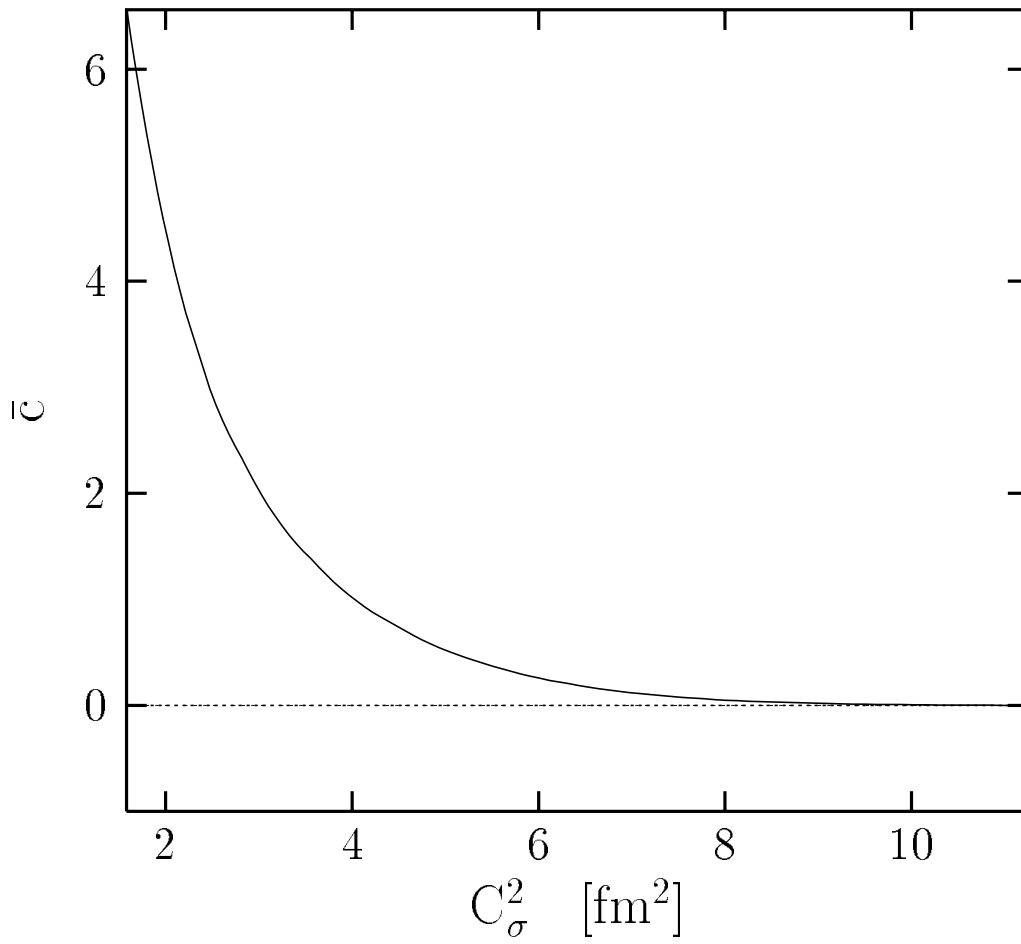


Fig.1  
The coupling parameter,  $\bar{c}$ , as a function of the coupling parameter  $C_\sigma^2$ .

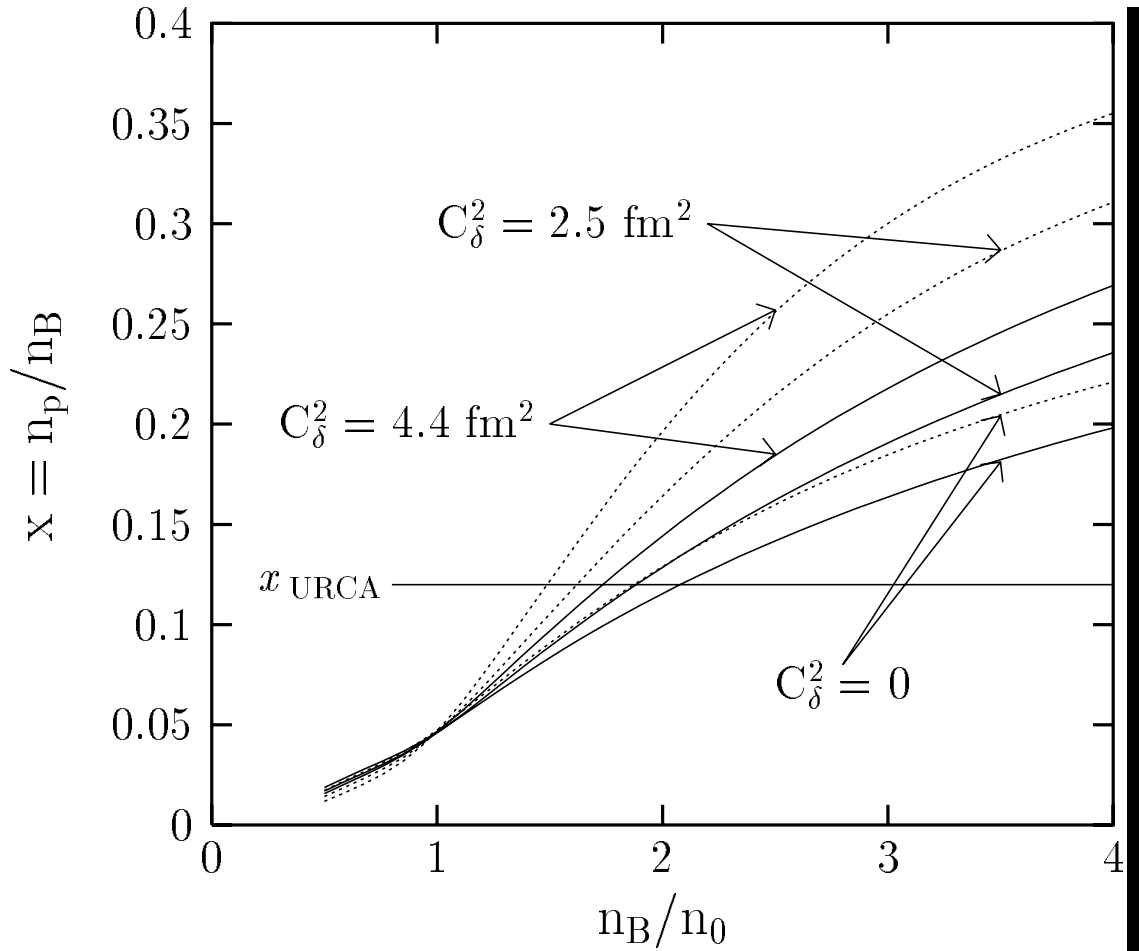


Fig.2  
 The proton fraction,  $x$ , of the neutron star matter for the soft EOS (solid curves) and the stiff EOS (dashed curves), for indicated values of the  $\delta$ -meson coupling,  $C_\delta^2$ .

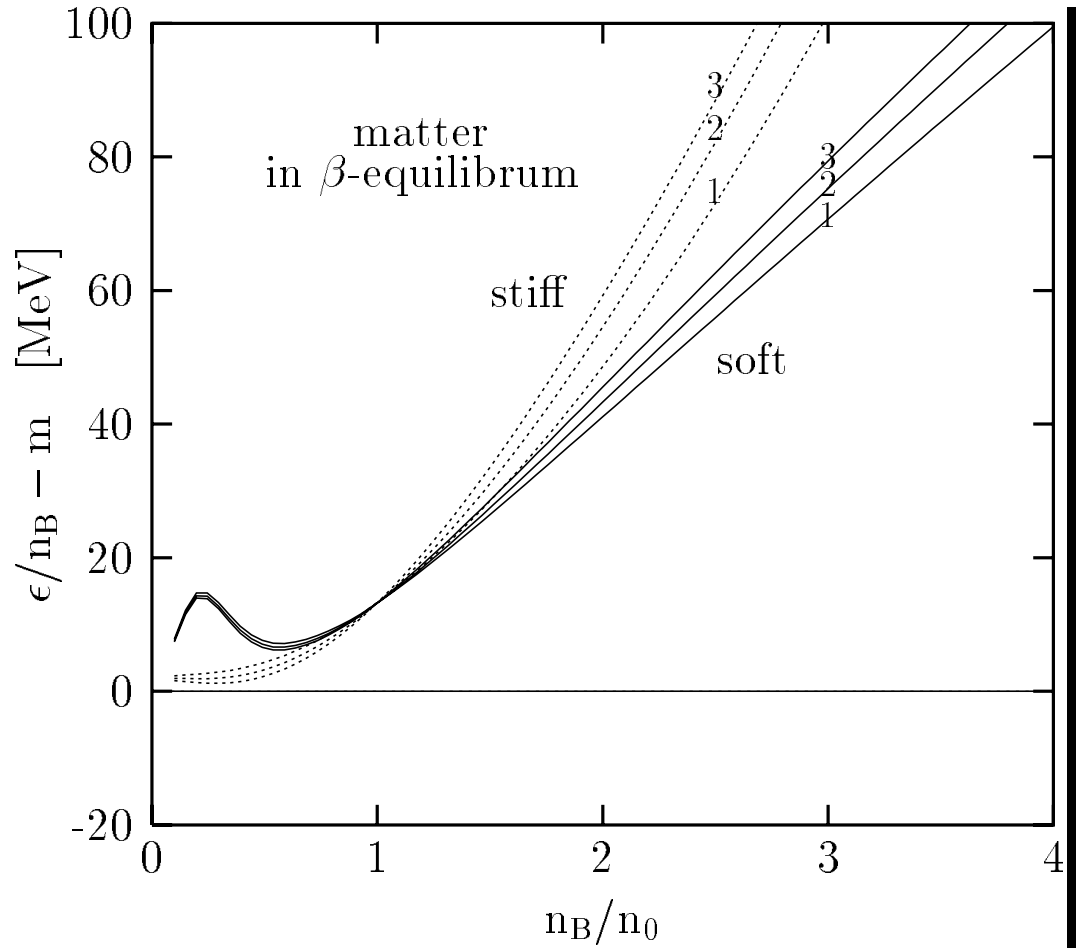
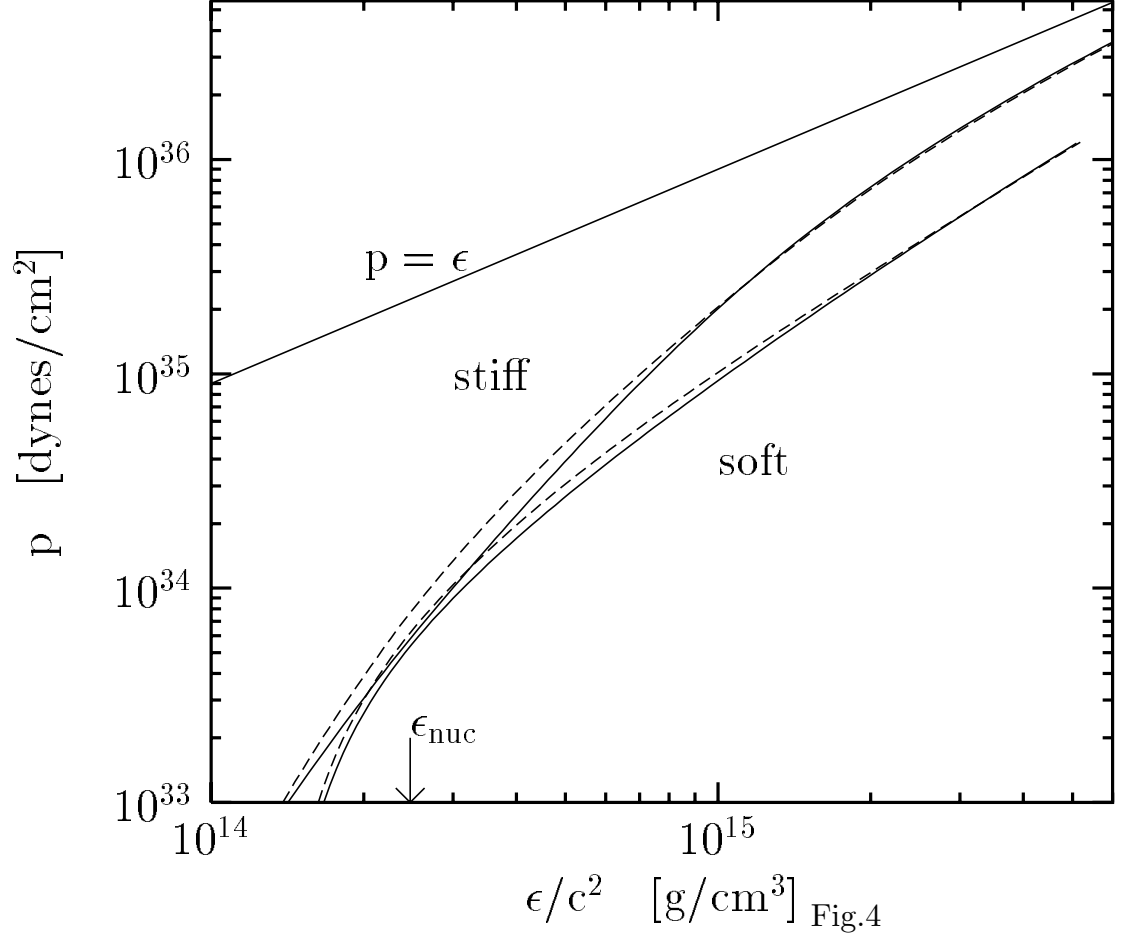


Fig.3

The energy per particle of the neutron star matter for the soft EOS and the stiff EOS. Curves labeled 1, 2, and 3 correspond, respectively, to  $C_\delta^2 = 0$ ,  $C_\delta^2 = 2.5 fm^2$ , and  $C_\delta^2 = 4.4 fm^2$ .



Pressure as a function of mass density for the soft EOS and the stiff EOS. Solid and dashed lines correspond, respectively, to  $C_\delta^2 = 0$  and  $C_\delta^2 = 4.4 fm^2$ .

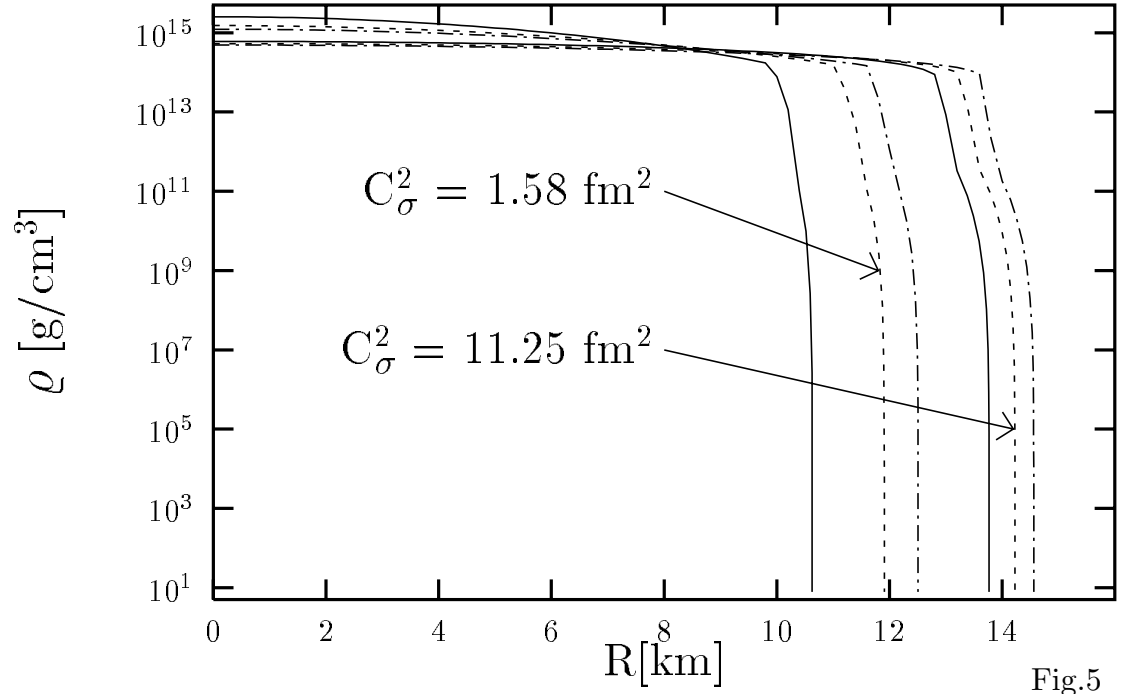


Fig.5

The density profile of  $1.4M_{\odot}$  neutron star for the soft EOS and for the stiff EOS. Solid, dashed and dotted-dashed lines correspond, respectively, to  $C_{\delta}^2 = 0$ ,  $C_{\delta}^2 = 2.5fm^2$ , and  $C_{\delta}^2 = 4.4fm^2$ .

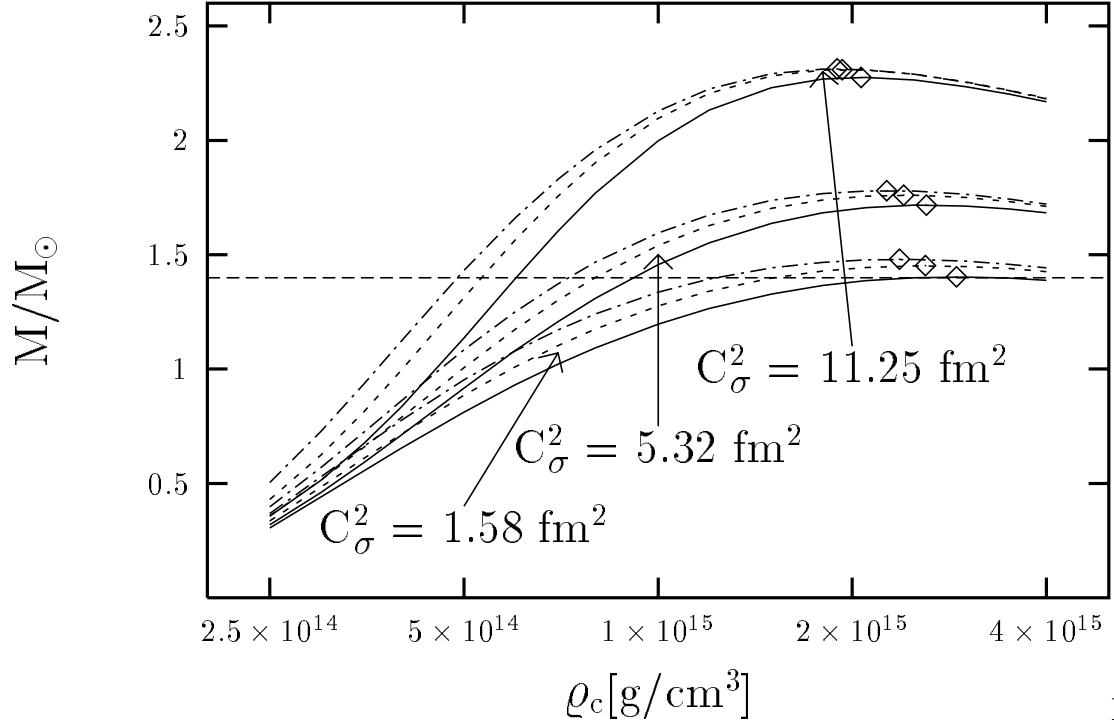


Fig.6

The spectrum of neutron star masses for the soft EOS and the stiff EOS. Also, results for the intermediate EOS are shown. Solid, dashed and dotted-dashed lines correspond, respectively, to  $C_{\delta}^2 = 0$ ,  $C_{\delta}^2 = 2.5 \text{ fm}^2$ , and  $C_{\delta}^2 = 4.4 \text{ fm}^2$ .